Forward−Backward Semiclassical Calculation of Spectral Line Shapes: I_2 in a Rare Gas Cluster

Oliver Kühn

Institut für Chemie, Physikalische und Theoretische Chemie, Freie Universität Berlin, Takustr. 3, 14195 Berlin, Germany

Nancy Makri*

School of Chemical Sciences, University of Illinois, 601 S. Goodwin Avenue, Urbana, Illinois 61801, and Theoretical and Physical Chemistry Institute, National Hellenic Research Foundation, 48 Vassileos Constantinou Avenue, Athens, Greece 11635

Received: June 7, 1999; In Final Form: July 19, 1999

The forward−backward semiclassical representation introduced by Makri and Thompson (*Chem. Phys. Lett.* **1998**, *291*, 101−109.) is employed to evaluate dipole correlation functions for electronic transitions of molecules in clusters or the condensed phase. The method is applied to the X → B transition of an iodine molecule in a host of argon atoms. In this case, where the spectrum is dominated by the short-time dynamics of the system, a factorization of the stability matrix entering the semiclassical expression of the propagator provides an excellent approximation, substantially reducing the computational cost.

1. Introduction

The microscopic description of condensed phase dynamics has provided a challenge over the past two decades. An exact quantum mechanical description of such processes as photoinduced reactive (photodissociation) and nonreactive (solvation) dynamics remains out of reach, as the numerical effort for solving the multidimensional Schrödinger equation grows exponentially with the number of coupled degrees of freedom. The alternative very appealing path integral description is plagued by the so-called sign problem which amounts to the inability of stochastic sampling methods to handle the integration of oscillatory functions.

In view of these difficulties inherent in quantum mechanical treatments of complicated many-body Hamiltonians, simplified models of the environment provide an attractive alternative. A popular description of many condensed phase processes is based on system−bath models. Here, the molecular system, i.e., a molecule in solution or in a solid state matrix, is mapped onto a low (one- or two-) dimensional system interacting with a bath which consists of uncoupled harmonic oscillators (see, for example, ref 1). The microscopic information about the bath and its interaction with the system is replaced by the spectral density function, a quantity which is often approximated by means of classical molecular dynamics simulations. Given the simplified system−bath Hamiltonian, the ensuing dynamics can be obtained either perturbatively[2−4] or exactly using numerical path integral methods.[5−12] Recent work has analyzed the conditions for validity of the system−bath description.[13] Clearly, the drawback in these formulations is the loss of microscopic information as a consequence of the mapping procedure. This has motivated efforts toward methods for dealing with large systems in full dimensionality, the most popular of which involve time-dependent mean field approximations,[14−16] mixed quantum-classical[17−19] and surface hopping schemes,[20−25] Gaussian wavepacket ideas,[26,27] and semiclassical approximations.[28−49] In addition, significant progress has been made in the direction of using the results of equilibrium path integral calculations via analytic continuation[50−53] and maximum entropy methods[54,55] or centroid density ideas[56−61] to deduce dynamical information. For recent reviews the reader is referred to refs 62 and 63.

In close analogy with the path integral situation,[64] Monte Carlo integration of the semiclassical propagator suffers from a phase cancellation problem due to its oscillatory character. A number of elegant methods for dealing with the semiclassical sign problem based on filtering procedures[38,39] or linearized approximations[41−43] have met with considerable success. An alternative, more rigorous approach[44−49] is based on the combined treatment of the forward and backward time evolution operators entering the influence functional or a correlation function. The forward−backward semiclassical dynamics (FBSD) method has the advantage that most of the rapid oscillations cancel and one is left with a smooth integrand.

In the present contribution we employ the FBSD scheme in the context of the spectroscopy of electronic transitions in the condensed phase. In section II we give a brief account of the theoretical apparatus. As phase cancellation is minimal in FBSD calculations, the most severe obstacle toward applying the method to large systems appears to be the computation of the prefactor, which scales as the third power of the number of atoms involved. We thus explore a simple factorization which substantially reduces the required computational effort associated with integrating the stability matrix. The specifics of the lineshape calculation are discussed in section III along with the numerical results that we obtained. The paper is finally summarized in section IV.

II. Theory

We focus on spectroscopic experiments described in terms of two electronic states, labeled g and e, which are coupled by

* Address correspondence to this author at the School of Chemical Sciences, University of Illinois, 601 S. Goodwin Avenue, Urbana, IL 61801.

10.1021/jp991836v CCC: $18.00
Published on Web 09/24/1999

the electromagnetic radiation field. Adopting the conventional classical treatment of the radiation field and the dipole approximation, the total Hamiltonian is written as

$$H(\mathbf{p},\mathbf{q}) = H_g(\mathbf{p},\mathbf{q})|g\rangle\langle g| + H_e(\mathbf{p},\mathbf{q})|e\rangle\langle e| - \mathbf{E}(t)\cdot(\boldsymbol{\mu}_{eg}(\mathbf{q})|e\rangle\langle g| + \boldsymbol{\mu}_{ge}(\mathbf{q})|g\rangle\langle e|) \quad (2.1)$$

Here $\mathbf{q}$ and $\mathbf{p}$ are Cartesian coordinates and momenta for the multidimensional system of interest, $\mathbf{E}(t)$ is the external electric field, and $\boldsymbol{\mu}_{ge}(\mathbf{q})$ is the dipole operator. Optical spectroscopy in weak external fields is conveniently described by employing a perturbation expansion of the time evolution operator with respect to the field (see, for example, ref 65). This results in expressions for the linear and nonlinear optical response functions in terms of dipole−dipole correlation functions. For instance, the linear absorption line shape normalized to unit area is given by the Fourier transform

$$\alpha(\omega) = \frac{1}{\pi}\mathrm{Re}\int_0^\infty dt\, e^{i\omega t}\, C(t) \quad (2.2)$$

where the dipole−dipole correlation function is

$$C(t) = \mathrm{Tr}[U_e(t)\boldsymbol{\mu}_{eg}(\mathbf{q})\rho_g U_g^{-1}(t)\cdot\boldsymbol{\mu}_{ge}(\mathbf{q})] \quad (2.3)$$

Here U_g and U_e are the time evolution operators of the ground and excited potential surfaces, respectively, ρ_g is the initial density operator prior to excitation, and the trace is taken with respect to the nuclear degrees of freedom. Assuming a thermal distribution of the molecular system of interest, the initial density is given by the Boltzmann operator,

$$\rho_g = Z^{-1}\exp(-\beta H_g) \quad (2.4)$$

where Z is the canonical partition function and $\beta = 1/k_B T$. Invoking the Condon approximation and setting $\boldsymbol{\mu}_{ge} = 1$, the correlation function takes the form

$$C(t) = \mathrm{Tr}(U_e(t)\rho_g U_g^{-1}(t)) \quad (2.5)$$

In the condensed phase the calculation of correlation functions of the type shown in eq 2.3 poses severe numerical difficulties unless one can resort to simple system−bath descriptions like the Brownian oscillator model which allows for an exact evaluation of (2.3) by using a cumulant expansion.[13] Although such mappings are justified in condensed phase situations under conditions that favor the validity of the linear response approximation, they are clearly inadequate for describing processes involving a few strongly interacting degrees of freedom such as those encountered in medium size clusters. The present article aims at describing a rigorous semiclassical methodology for dealing with the spectroscopy of such systems, treating the potential interactions in full dimensionality.

The semiclassical propagator in the coordinate representation can be obtained by applying the stationary phase approximation to the path integral.[66,67] The result, first obtained by Van Vleck[28] by a different method, involves a phase equal to the action along classical trajectories connecting the initial and final points and a prefactor which amounts to contributions from quadratic fluctuations about a classical path. The endpoint representation is not useful for the purpose of performing numerical calculations as the determination of the relevant trajectories requires the solution of a double ended boundary value problem. This numerical difficulty is overcome in initial value representations of time correlation functions which replace the integration over final coordinates by one involving initial momenta[30] or invoke cellular discretizations[34] or coherent state representations.[32] In these formulations, the classical trajectories are specified by their initial conditions in phase space. A number of successful applications to small model[35,36] and chemical systems[39,49,68] have demonstrated the high accuracy of the semiclassical approximation as well as some of its limitations. In addition, semiclassical ideas have been successfully combined with quantum-classical approaches to treat polyatomic systems.[69−71] Multidimensional calculations require integration by Monte Carlo methods which (because of the oscillatory phase present in the semiclassical integrand) are plagued by a sign problem very similar to that encountered in real-time path integration. Even though a few successful calculations employing filtering procedures[38,39] or linearization approximations[41,42] have been reported, rigorous semiclassical calculations in large systems have in the past been considered unfeasible.

In previous attempts to develop a semiclassical representation of (2.5) and its obvious generalization to nonlinear spectroscopies the forward and backward propagation has been treated separately while the integrals associated with switching between electronic states that appear in higher order terms were performed within the stationary phase approximation.[72−75]

In ref 72 this procedure was combined with a harmonic expansion around the center of the classical orbits of the forward and backward trajectories in the spirit of Gaussian wave packet and cellular dynamics[34] with application to an electronic two-level system coupled to a single nuclear coordinate. Spencer and Loring[74] treated a solute in a Lennard-Jones solvent semiclassically, simplifying matters by neglecting the amplitude of the semiclassical propagator. They also discussed the shortcomings of semiclassical approaches which reduce the correlation function to the ground or excited state dynamics of the instantaneous energy gap.

To circumvent the difficulty associated with the oscillatory nature of the semiclassical propagator, Makri and Thompson formulated a FBSD scheme for ensemble-averaged quantities.[44,46,47] The main idea is to apply the semiclassical approximation to the combined forward and reverse time evolution operators. After reaching the desired propagation time, trajectories are subsequently propagated back to time zero, such that the net accumulated action is generally small. This fact implies that the semiclassical integrand is now only mildly oscillatory, allowing Monte Carlo sampling. Batista et al.[49] have used this scheme to simulate the photoelectron spectrum of I_2^- in the gas phase.

References 44 and 46 present in detail the FBSD scheme for the influence functional arising from coupling of a multidimensional medium to a time-dependent system. Equation 2.5 for the correlation function pertinent to the photoabsorption spectrum has exactly the same structure, the forward and backward evolution operators now involving the forces on the ground and excited potential surfaces. For this purpose, we simply rewrite the result of refs 44 and 46 in the present notation:

$$C(t) = (2\pi\hbar)^{-n}\int d\mathbf{p}_0 \int d\mathbf{q}_0\, D(\mathbf{q}_0,\mathbf{p}_0)\times \exp\left(\frac{i}{\hbar}S(\mathbf{q}_0,\mathbf{p}_0)\right)\langle G(\mathbf{q}_0,\mathbf{p}_0)|\rho_g|G(\mathbf{q}_f,\mathbf{p}_f)\rangle \quad (2.6)$$

Here

$$G(\mathbf{q}_0,\mathbf{p}_0) = \left(\frac{2}{\pi}\right)^{n/4} (\det \boldsymbol{\gamma})^{1/4} \times \exp\left(-(\mathbf{q}-\mathbf{q}_0)\cdot\boldsymbol{\gamma}\cdot(\mathbf{q}-\mathbf{q}_0) + \frac{i}{\hbar}\mathbf{p}_0\cdot(\mathbf{q}-\mathbf{q}_0)\right) \quad (2.7)$$

where $\boldsymbol{\gamma}$ is a diagonal matrix, defines a multidimensional coherent state. According to eq 2.6, trajectories are chosen with initial conditions $\mathbf{q}_0,\mathbf{p}_0$ based on weights given by the coherent state transform of the initial density operator. These trajectories are first propagated to time t according to the ground state Hamiltonian and subsequently return to zero time following the forces in the excited electronic state. Finally, S is the net action during this forward−backward evolution, i.e.

$$S(\mathbf{q}_0,\mathbf{p}_0) = \int_0^t (\mathbf{p}(t')\cdot\dot{\mathbf{q}}(t') - H_e)\, dt' + \int_t^0 (\mathbf{p}(t')\cdot\dot{\mathbf{q}}(t') - H_g)\, dt' \quad (2.8)$$

The main advantage of the FBSD formulation in the context of propagation in a single electronic state[12,13] is that the combined forward−backward action tends to be small on the scale of Planck's constant and thus the integrand is only mildly oscillatory. In the present context, the extent of forward−backward cancellation depends on how different the ground and excited state Hamiltonians are. In the limit $H_g = H_e$, the forward and backward propagation steps cancel exactly and the corresponding action is identically equal to zero. The prefactor in (2.6) is given by $D(\mathbf{q}_0,\mathbf{p}_0) = \sqrt{\det\mathbf{M}}$ with the matrix $\mathbf{M}$ defined in terms of the elements of the stability matrix

$$M_{ij} = \frac{1}{2}\left(\frac{\partial q_{j,f}}{\partial q_{i,0}} + \frac{\gamma_i}{\gamma_j}\frac{\partial p_{j,f}}{\partial p_{i,0}} - 2i\hbar\gamma_i\frac{\partial q_{j,f}}{\partial p_{i,0}} + \frac{i}{2\hbar\gamma_j}\frac{\partial p_{j,f}}{\partial q_{i,0}}\right) \quad (2.9)$$

To calculate the determinant, one needs to solve the $(2n)^2$ differential equations for these elements. Having in mind applications to large systems, the quadratic scaling of this procedure becomes the bottleneck. For this reason we will also explore the validity of the simplest approximation in which the correlations between initial and final phase space points of different degrees of freedom are neglected, i.e. $M_{ij} \approx \delta_{ij}M_{ii}$. In this approximation, the prefactor D is replaced by $D_{fact} = [\prod_i M_{ii}]^{1/2}$.

Finally, we mention how the FBSD treatment described in this section can be used to evaluate the dipole correlation function without invoking the Condon approximation. For this purpose, eq 2.5 is written in the form

$$C(t) = -i\frac{\partial}{\partial\mathbf{z}}\cdot \mathrm{Tr}(\boldsymbol{\mu}_{eg}(\mathbf{q})\rho_g U_g^{-1}(t) e^{i\mathbf{z}\cdot\boldsymbol{\mu}_{ge}(\mathbf{q})} U_e(t))|_{\mathbf{z}=0} \quad (2.10)$$

The product of the three last operators in this expression can be interpreted as propagation with the following time-dependent Hamiltonian:[45,48]

$$\tilde{H}(t') \equiv H - \hbar\mathbf{z}\cdot\boldsymbol{\mu}\delta(t'-t) \quad (2.11)$$

The classical dynamics generated by this effective Hamiltonian are described by Hamilton's equations,

$$\dot{\mathbf{q}}(t') = \frac{\partial\tilde{H}}{\partial\mathbf{p}} = \frac{\partial H}{\partial\mathbf{p}}, \quad \dot{\mathbf{p}}(t') = -\frac{\partial\tilde{H}}{\partial\mathbf{q}} = -\frac{\partial H}{\partial\mathbf{q}} + \hbar\frac{\partial\boldsymbol{\mu}}{\partial\mathbf{q}}\cdot\mathbf{z}\delta(t-t') \quad (2.12)$$

According to these, the momentum of each trajectory must jump at time t by the amount

$$\delta\mathbf{p} = \hbar\frac{\partial\boldsymbol{\mu}}{\partial\mathbf{q}}\cdot\mathbf{z} \quad (2.13)$$

The action generated by the Hamiltonian of eq 2.11 also increments discontinuously at the time t by the amount

$$\delta S = \hbar\boldsymbol{\mu}(t)\cdot\mathbf{z} \quad (2.14)$$

Application of the semiclassical approximation to the effective Hamiltonian in the coherent state representation brings the correlation function to the form

$$C(t) = -i(2\pi\hbar)^{-1}\frac{\partial}{\partial\mathbf{z}}\cdot\int d\mathbf{q}_0 \int d\mathbf{p}_0 D(\mathbf{q}_0,\mathbf{p}_0) \times \exp\left(\frac{i}{\hbar}S(\mathbf{q}_0,\mathbf{p}_0)\right)\langle G(\mathbf{q}_0,\mathbf{p}_0)|\rho_g\boldsymbol{\mu}|G(\mathbf{q}_f,\mathbf{p}_f)\rangle|_{\mathbf{z}=0} \quad (2.15)$$

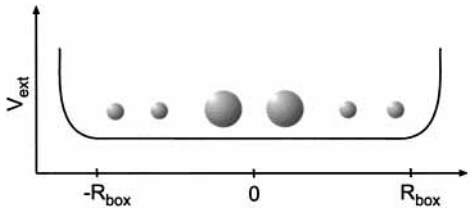

Figure 1. Linear chain configuration of I_2 (large spheres) in an Ar (small spheres) environment. The system is placed in a box introduced via the external potential $V_{ext}(\mathbf{q})$. The latter is taken as the repulsive part of the Ar−Ar Lennard-Jones potential thus modeling the presence of further Ar atoms.

III. Application to I_2 in an Ar cluster

The photodissociation of I_2 in a cluster environment has been an active testing ground for new theoretical propagation methods. Gerber and co-workers applied their classical separable potential based approach to this system calculating absorption and resonance Raman spectra.[76,77] A so-called mixed-order semiclassical approach combining zeroth- and second-order approximations to the propagator has been used by Ovchinnikov et al. to obtain the absorption, emisson, and resonance Raman profiles for I_2 in solid Kr.[70,78]

Much effort has also been invested in the theoretical simulation of pump−probe spectra which show a pronounced pressure dependence.[79,80] Purely classical molecular dynamics simulations,[79,81] and quantum/classical hybrid methods,[82,83] as well as the combination of quantum propagation for the early time dynamics with classical simulations for later times[84] have added much to the understanding of the relaxation/recombination dynamics in this system.

In this section we apply the FBSD expression for the linear absorption correlation function to the spectroscopy of the X → B electronic transition of an iodine molecule embedded in a cluster of argon atoms at finite temperature. In the absence of detailed information for the dipole moment function we restrict ourselves to the Condon approximation. Nonadiabatic transitions within the I_2 excited electronic state manifold do not play a significant role for the linear absorption profile[77] and therefore will be neglected. Further, to keep the matter simple we restrict ourselves to a linear chain configuration (see Figure 1) as has been done for the present system in[82,83] and for the I_2 anion in Ar and Xe in refs 82 and 83.

The Cartesian coordinates and momenta of the two iodine atoms are denoted $\mathbf{r}_i$ and $\mathbf{p}_i$ ($i = 1, 2$), respectively, while those of the n Ar atoms are written as $\mathbf{R}_j$, $\mathbf{P}_j$ ($j = 1, ..., n$). In the actual calculation we will describe the solute by its relative (bond

TABLE 1: Parameters of the Morse Potential Describing the Ground and Excited States of I_2 (from Ref 79)

	D (cm^{-1})	λ (Å^{-1})	b (Å)	d (cm^{-1})
ground state	12547.2	1.875	2.656	0
excited state	4382.8	1.75	3.03	7605

distance) and center of mass coordinates $\tilde{\mathbf{r}}$ and $\mathbf{R}_0$, respectively. The respective conjugate momenta are $\tilde{\mathbf{p}}$ and $\mathbf{P}_0$. Employing a pairwise additive potential, the Hamiltonian takes the form

$$H = H_{I_2} + H_{sol} \tag{3.1}$$

where

$$H_{I_2} = \frac{\tilde{p}^2}{2\mu_{I-I}} + V_{I-I}(\tilde{r}) \tag{3.2}$$

describes the internal vibration of the iodine molecule and

$$H_{sol} = \sum_{i=1}^{n}\frac{\mathbf{P}_i^2}{2m_{Ar}} + \sum_{i>j}^{n} V_{Ar-Ar}(|\mathbf{R}_i - \mathbf{R}_j|) + \sum_{i=1}^{n} V_{I-Ar}(|\mathbf{r}_1 - \mathbf{R}_i|) + \sum_{i=1}^{n} V_{I-Ar}(|\mathbf{r}_2 - \mathbf{R}_i|) + \frac{\mathbf{P}_0^2}{4m_1} + V_{ext}(\mathbf{R}_0...\mathbf{R}_n) \tag{3.3}$$

is the Hamiltonian of the argon atoms and their interactions with the iodine molecule as well as the overall translation of the latter. The ground and excited-state potentials for I_2, Ar−Ar, and the I−Ar interaction are taken from ref 79. Specifically, the vibrational motion of I_2 is described by a Morse potential of the form

$$V_{I-I}(\tilde{r}) = D[\exp(-2\lambda(\tilde{r} - b)) - 2\exp(-\lambda(\tilde{r} - b))] + d$$

and the Ar−Ar and I−Ar interaction potentials are of the Lennard-Jones type:

$$V_{LJ}(\delta R) = 4\epsilon\left[\left(\frac{\sigma}{\delta R}\right)^{12} - \left(\frac{\sigma}{\delta R}\right)^{6}\right]$$

with no distinction made for the ground and excited state of I_2. The parameters of these potentials are given in Tables 1 and 2. To mimic the effect of additional solvent atoms the system is placed in a box of length $2R_{box}$ (see Figure 1). For the external box potential entering eq 3.3, we chose the repulsive part of the Lennard-Jones potential with the parameters for the Ar−Ar interaction.

The initial density operator is approximated by the product

$$\rho(0) \approx \exp(-\beta H_{sol})|\psi_{I_2}\rangle\langle\psi_{I_2}| \tag{3.4}$$

where $\psi_{I_2}(\tilde{r})$ is the wave function of the iodine molecule in the vibrational ground state of the ground electronic state. Note that H_{sol} is evaluated in eq 3.4 with the iodines fixed at their ground state equilibrium position. For simplicity, the ground state wave function for the solute is approximated by a Gaussian form,

$$\psi_{I_2}(\tilde{r}) = \left(\frac{2\alpha}{\pi}\right)^{1/4}\exp\{-\alpha(\tilde{r} - \tilde{r}_{eq})^2\} \tag{3.5}$$

where $\tilde{r}_{eq}$ is the equilibrium bond length.

Since the Ar atoms are fairly heavy, we use the high-temperature approximation to calculate the solvent part of the Boltzmann matrix element. The density matrix elements in the coherent state representation have been given in refs 12 and 13. With these assumptions the correlation function becomes

$$C(t) = 2^{3(n+2)}\prod_{k=1}^{n}\int d\mathbf{R}_{k,0}\int d\mathbf{P}_{k,0}\int d\mathbf{Q}_k\int d\mathbf{r}_{1,0}\int d\mathbf{p}_{1,0}\int d\mathbf{r}_{2,0}\int d\mathbf{p}_{2,0}\, D(\mathbf{r}_{1,0},\mathbf{p}_{1,0},\mathbf{r}_{2,0},\mathbf{p}_{2,0},\mathbf{R}_{k,0},\mathbf{P}_{k,0}) \times f_{norm}(\mathbf{r}_{1,0},\mathbf{p}_{1,0},\mathbf{r}_{2,0},\mathbf{p}_{2,0},\mathbf{R}_{k,0},\mathbf{P}_{k,0},\mathbf{Q}_k) \times \exp\left(\frac{i}{\hbar}S(\mathbf{r}_{1,0},\mathbf{p}_{1,0},\mathbf{r}_{2,0},\mathbf{p}_{2,0},\mathbf{R}_{k,0},\mathbf{P}_{k,0})\right) \times \exp\left(-\sum_{k=1}^{n}\frac{m_k}{m_k + \hbar^2\beta\gamma_k}\left(\frac{\beta}{4m_k}\mathbf{P}_{k,f}^2 + \gamma_k\left|\mathbf{Q}_k - \mathbf{R}_{k,f}\right|^2 + \frac{i}{\hbar}\mathbf{Q}_k\cdot(\mathbf{P}_{k,0} - \mathbf{P}_{k,f}) - \frac{i}{\hbar}(\mathbf{P}_{k,0}\cdot\mathbf{R}_{k,0} - \mathbf{P}_{k,f}\cdot\mathbf{R}_{k,f})\right)\right) \times \exp\left(-\frac{\alpha\gamma_0}{\alpha+\gamma_0}\left|\tilde{\mathbf{r}}_f - \tilde{\mathbf{r}}_{eq}\right|^2 - \frac{\tilde{p}_f^2}{4(\alpha+\gamma_0)} - \frac{i}{\hbar}\frac{\alpha}{\alpha+\gamma_0} \times (\tilde{\mathbf{p}}_0\cdot(\tilde{\mathbf{r}}_0 - \tilde{\mathbf{r}}_{eq}) - \tilde{\mathbf{p}}_f\cdot(\tilde{\mathbf{r}}_f - \tilde{\mathbf{r}}_{eq}))\right) \tag{3.6}$$

In the above equation, $\mathbf{Q}_k$ are auxiliary integration variables arising from the coherent state transform of the Boltzmann operator in the high-temperature approximation, and the normalized sampling function is given by the expression

$$f_{norm}(\mathbf{r}_{1,0},\mathbf{p}_{1,0},\mathbf{r}_{2,0},\mathbf{p}_{2,0},\mathbf{R}_{k,0},\mathbf{P}_{k,0},\mathbf{Q}_k) = \exp\left(-\sum_{k=1}^{n}\frac{m_k}{m_k + \hbar^2\beta\gamma_k}\left(\frac{\beta}{4m_k}\mathbf{P}_{k,0}^2 + \gamma_k\left|\mathbf{Q}_k - \mathbf{R}_{k,0}\right|^2\right) - \frac{\alpha\gamma_0}{\alpha+\gamma_0}\left|\tilde{r}_0 - \tilde{r}_{eq}\right|^2 - \frac{\tilde{p}_0^2}{4(\alpha+\gamma_0)}\right) \tag{3.7}$$

Details of the Monte Carlo procedure are discussed in ref 46.

We start our discussion by assessing the importance of correlations in the calculation of the determinant prefactor D in eq 3.6. In Figure 2 we plot a set of trajectories for the case of four Ar atoms. The initial conditions have been taken from a Monte Carlo sampling step at $T = 300$ K. The solute is in the excited state; i.e., the trajectories correspond to the forward propagation. The elements of the stability matrix entering eq 2.9 have been calculated by running for each selected set of initial conditions concurrent trajectories with slightly modified initial values such as to allow for a finite difference approximation to the derivatives in (2.9). The integration of the classical equations of motion was performed using the velocity Verlet algorithm.[85]

Apparently, on the time scale covered in Figure 2 the factorized approximation is very accurate for these trajectories. As can be seen from the upper panel the deviation is only about 4% within the first 700 fs. Note that initially the I_2 is compressed to an extent that the energy on the excited state is above the dissociation threshold for this bond. The initial momenta are zero for all particles.

In Figure 3 we show a situation where the factorization approximation completely breaks down at longer times. From the forward trajectories propagated on the excited solute state the reason for this break down does not become obvious.

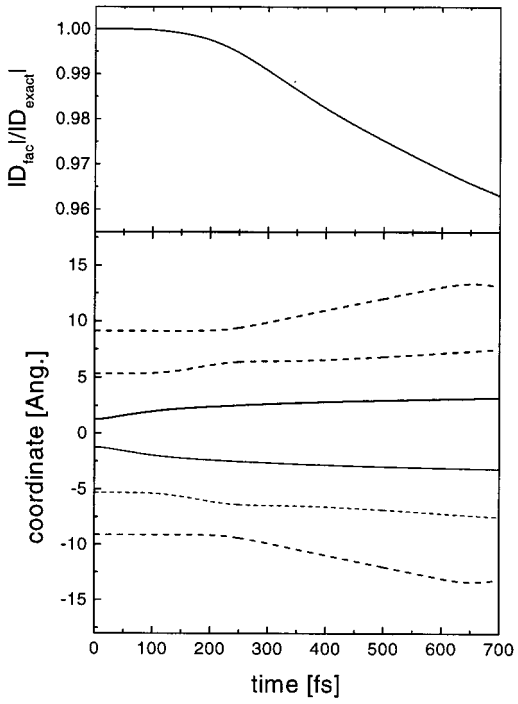

Figure 2. Classical trajectories and semiclassical prefactor for a linear chain of I_2 plus four Ar atoms. The solute dynamics is on the excited state (forward propagation). The external confining potential starts at $R_{box} = 14.6$ Å. This corresponds to the situation where for I_2 in the ground state the equilibrium I−Ar and Ar−Ar distances are equal to the Lennard-Jones minimum $2^{1/6}\sigma$. The initial conditions for the trajectories are taken from an arbitrary step in the Monte Carlo sampling of the integrals in eq 3.6. With this initial condition the forward and backward parts of the trajectories are nearly indistinguishable. The lower panel shows the coordinates of the I atoms (solid lines) and those of the Ar atoms (dashed lines). The upper panel shows the ratio between the absolute values of the factorized and the exact determinant.

TABLE 2: Parameters of the Lennard-Jones Potentials Describing the I−Ar and Ar−Ar Interactions (from Ref 79)

	ϵ (cm^{-1})	σ (Å)
I−Ar	209.7	3.59
Ar−Ar	84.0	3.40

However, if one inspects the complete forward−backward trajectory as is done for the final time (700 fs) in the lower panel of Figure 3, the reason for the failure of the factorization approximation becomes transparent. Tracing their backward motion on the I_2 ground state, one observes an intramolecular I_2 collision and the attraction between an iodine and a neighboring Ar atom. These cause the final phase space points of the involved particles to become correlated, in contrast to the case shown in Figure 2 where the backward ground state trajectory traced the forward trajectory almost exactly for a final time of 700 fs. Figure 3 also suggests that one can improve the factorization approximation by including correlations between neighboring particles, for instance, those in the first solvation shell surrounding the solute. In this case the matrix (2.9) would take a block-diagonal form; the resulting ratio $|D_{approx}|/|D_{exact}|$ is shown as the dashed line in the upper panel of Figure 3. Including also the next-nearest-neighbor interaction with the Argon atom whose trajectory starts at about −8 Å accounts for most of the correlations in the time interval examined (thin solid line in upper panel of Figure 3).

The broad absorption spectrum of I_2 is dominated by the short-time dynamics of the system. As shown, for example, in ref 39, the ground state wave packet once promoted to the

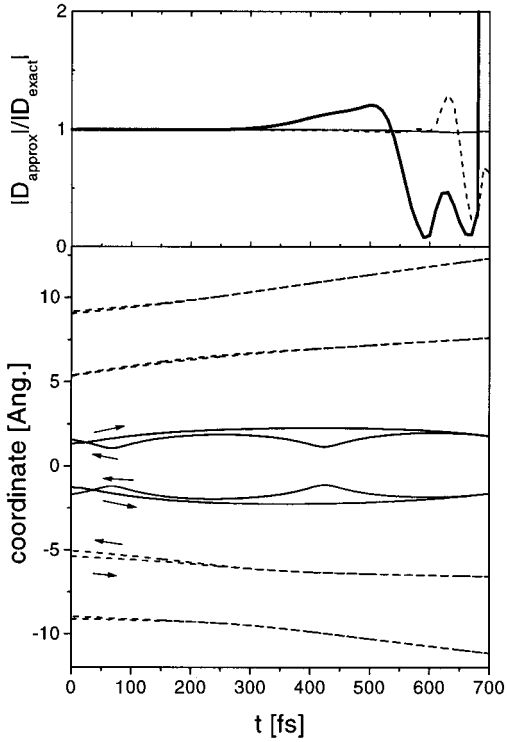

Figure 3. Same as in Figure 2 but for a different set of initial conditions. In addition to the forward trajectories on the I_2 excited state, the backward parts of the trajectories on the ground states are shown for the longest forward propagation time. The respective directions are indicated by arrows. In the upper panel the determinant for the full factorization (thick solid line) and block diagonal approximation (dashed: only first solvation shell; thin solid: additional inclusion of the argon whose trajectory starts at about −8 Å) is compared to the exact determinant according to eq 2.9.

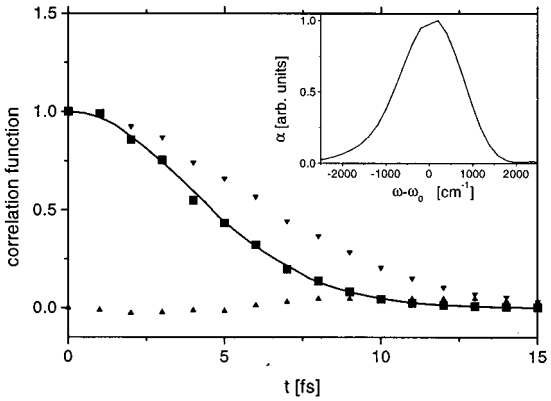

Figure 4. Comparison between the exact gas phase (solid line) and the FBSD condensed phase results (markers) for the correlation function of the X → B state Franck−Condon transition at room temperature. The triangles show the real and imaginary parts of the correlation function. The inset shows the spectrum taken with respect to the vertical transition frequency ω_0.

excited state leaves the Franck−Condon region in about 15 fs. On this time scale the factorization approximation should perform rather well, judging from the two extreme cases shown in Figures 2 and 3. In Figure 4 we plot the correlation function for the I_2 plus four Ar atoms system using the factorized determinant. For each integration variable in eq 3.6 35 000 Monte Carlo points have been sampled with a rejection ratio for the Metropolis random walk of 50%. It turns out that the correlation function is nearly identical to the gas phase result which has been obtained by calculating the overlap $\langle\psi_{I_2}|\exp(-iH_e t/\hbar)|\psi_{I_2}\rangle$ using the standard split-operator technique in

conjunction with a fast Fourier transform scheme for calculating the action of the kinectic energy operator.[86] This finding is in line with the fact that the spectrum is determined by the short-time dynamics in the Franck−Condon region where the gas phase potentials are not substantially altered by the interaction with the rare gas environment.

IV. Summary

The FBSD scheme for calculating correlation functions offers a straightforward and practical methodology for studying the dynamics and spectroscopy of polyatomic molecules and clusters. In the Condon approximation, the correlation function for the linear absorption spectrum involves a time evolution on the excited potential surface followed by reverse propagation on the ground state Hamiltonian. Combining both steps into a single semiclassical evolution eliminates the most severe oscillations of each separate semiclassical propagator, giving rise to a smooth integrand that invites the use of Monte Carlo methods. We have also discussed how the scheme can be formulated without reference to the Condon approximation. Furthermore, combination of the FBSD idea a stationary phase state switching procedure[72−75] will lead to a powerful methodology for simulating nonlinear spectroscopies.

In the present paper we applied the FBSD procedure to calculate the absorption spectrum for the X → B transition of iodine embedded in a cluster of four argon atoms in a linear arrangement. In this case the spectrum is dominated by the short time dynamics of I_2, which dissociates very rapidly once promoted to the excited B surface. As a consequence, the interaction with the Ar environment plays a minor role in determining the spectrum. Nevertheless, the present results obtained via the full semiclassical method are useful as benchmarks since the present system continues to serve as a testing ground for less rigorous approximations. It will be challenging to apply the FBSD methodology to other situations where persisting recurrences in the correlation function give rise to vibrational structure, while interaction with the medium results in line-shape broadening.

As the FBSD methodology reduces dramatically the severity of the Monte Carlo sign problem encountered in path integral or single-direction semiclassical treatments, the major computational overhead of the method is associated with the determinant prefactor. The latter requires costly propagation of the stability matrix as well as the evaluation of a determinant that scales as the third power of the number of degrees of freedom. In the present work we explored a few ways of simplifying this procedure. Full factorization of the determinant leads to an extremely efficient algorithm that reproduces the short-time dynamics rather faithfully. At longer times binary collisions become important and the factorization scheme breaks down. We found that following the full stability matrix of the solute plus one solvation shell leads to significant improvement while resulting in an economical block-diagonal form. Finally, we expect that inclusion of off-diagonal terms between neighboring atoms only will offer further increase in accuracy at little additional cost, as the resulting stability matrix will be tridiagonal. These procedures offer a promising starting point but further tests will be needed to establish the most fruitful approach to the semiclassical dynamics of polyatomic systems.

Acknowledgment. O.K. gratefully acknowledges financial support by the Deutsche Forschungsgemeinschaft (project Ku952/2-1). N.M. thanks the Packard Foundation and the National Science Foundation for supporting this work and the Faculty of the National Hellenic Research Foundation for their hospitality during her sabbatical stay. We also thank Dr. Keiran Thompson for an early version of the code and useful discussions.

References and Notes

(1) May, V.; Kühn, O. *Theory of charge and energy transfer in molecular systems*; Wiley: New York, 1999.
(2) Jean, J.; Friesner, R. A.; Fleming, G. R. *J. Chem. Phys.* **1992**, *96*, 5827.
(3) Kohen, D.; Marston, C. C.; Tannor, D. J. *J. Chem. Phys.* **1997**, *107*, 5236−5253.
(4) Pollard, W. T.; Felts, A. K.; Friesner, R. A. *Adv. Chem. Phys.* **1996**, *XCIII*, 77.
(5) Makri, N. *Chem. Phys. Lett.* **1992**, *193*, 435−444.
(6) Makri, N.; Makarov, D. E. *J. Chem. Phys.* **1995**, *102*, 4600−4610.
(7) Makri, N.; Makarov, D. E. *J. Chem. Phys.* **1995**, *102*, 4611−4618.
(8) Sim, E.; Makri, N. *Comput. Phys. Commun.* **1997**, *99*, 335−354.
(9) Makri, *J. Phys. Chem.* **1998**, *102*, 4414−4427.
(10) Mak, C. H. *Phys. Rev. Lett.* **1992**, *68*, 899−902.
(11) Mak, C. H.; Egger, R. *Phys. Rev. E* **1994**, *49*, 1997−2008.
(12) Mak, C. H.; Egger, R. *Adv. Chem. Phys.* **1996**, *XCIII*, 39−76.
(13) Makri, N. *J. Phys. Chem.* **1999**, *103*, 2823−2829.
(14) Dirac, P. A. *Proc. Cambridge Philos. Soc.* **1930**, *26*.
(15) Heller, E. J. *J. Chem. Phys.* **1976**, *64*, 63−73.
(16) Harris, R. *J. Chem. Phys.* **1980**, *72*, 1776.
(17) Mittleman, M. H. *Phys. Rev.* **1961**, *122*, 499.
(18) Gerber, R. B.; Buch, V.; Ratner, M. A. *J. Chem. Phys.* **1982**, *77*, 3022−3030.
(19) Wahnstrom, G.; Carmeli, B.; Metiu, H. *J. Chem. Phys.* **1988**, *88*, 2478−2491.
(20) Tully, J. C.; Preston, R. K. *J. Chem. Phys.* **1971**, *55*, 562−572.
(21) Tully, J. C. *J. Chem. Phys.* **1990**, *93*, 1061−1071.
(22) Hammes-Schiffer, S.; Tully, J. C. *J. Chem. Phys.* **1994**, *101*, 4657−4667.
(23) Hammes-Schiffer, S. *J. Chem. Phys.* **1996**, *105*, 2236.
(24) Space, B.; Coker, D. F. *J. Chem. Phys.* **1992**, *96*, 652−663.
(25) Coker, D. F.; Xiao, L. *J. Chem. Phys.* **1995**, *102*, 496−510.
(26) Heller, E. J. *J. Chem. Phys.* **1975**, *62*, 1544−1555.
(27) Heller, E. J. *J. Chem. Phys.* **1981**, *75*, 2923−2930.
(28) Van Vleck, J. H. *Proc. Nat. Acad. Sci. U.S.A.* **1928**, *14*, 178.
(29) Morette, C. *Phys. Rev.* **1952**, *81*, 848.
(30) Miller, W. H. *Adv. Chem. Phys.* **1974**, *25*, 69.
(31) Miller, W. H. *Adv. Chem. Phys.* **1975**, *30*, 77.
(32) Herman, M. F.; Kluk, E. *Chem. Phys.* **1984**, *91*, 27−34.
(33) Kluk, E.; Herman, M. F.; Davis, H. L. *J. Chem. Phys.* **1986**, *84*, 326−334.
(34) Heller, E. J. *J. Chem. Phys.* **1991**, *94*, 2723.
(35) Tomsovic, S.; Heller, E. J. *Phys. Rev. Lett.* **1991**, *67*, 664−667.
(36) Sepulveda, M. A.; Tomsovic, S.; Heller, E. J. *Phys. Rev. Lett.* **1992**, *69*, 402−405.
(37) Herman, M. F. *Annu. Rev. Phys. Chem.* **1994**, *45*, 83.
(38) Walton, A. R.; Manolopoulos, D. E. *Mol. Phys.* **1996**, *84*, 961.
(39) Brewer, M. L.; Hulme, J. S.; Manolopoulos, D. E. *J. Chem. Phys.* **1997**, *106*, 4832−4839.
(40) Sun, X.; Miller, W. H. *J. Chem. Phys.* **1997**, *106*, 6346−6353.
(41) Wang, H.; Sun, X.; Miller, W. H. *J. Chem. Phys.* **1998**, *108*, 9726−9736.
(42) Sun, X.; Wang, H.; Miller, W. H. *J. Chem. Phys.* **1998**, *109*, 4190−4200.
(43) Sun, X.; Wang, H.; Miller, W. H. *J. Chem. Phys.* **1998**, *109*, 7064−7074.
(44) Makri, N.; Thompson, K. *Chem. Phys. Lett.* **1998**, *291*, 101−109.
(45) Miller, W. H. *Faraday Discuss.* **1998**, *110*, 1−21.
(46) Thompson, K.; Makri, N. *J. Chem. Phys.* **1999**, *110*, 1343−1353.
(47) Thompson, K.; Makri, N. *Phys. Rev. E* **1999**, *59*, R4729−R4732.
(48) Shao, J.; Makri, N. *J. Phys. Chem.* submitted for publication.
(49) Batista, V.; Zanni, M. T.; Greenblatt, J.; Neumark, D. M.; Miller, W. H. *J. Chem. Phys.* **1999**, *110*, 3736−3747.
(50) Thirumalai, D.; Berne, B. J. *J. Chem. Phys.* **1984**, *81*, 2512−2513.
(51) Thirumalai, D.; Berne, B. J. *Comput. Phys. Commun.* **1991**, *63*, 415−426.
(52) Behrman, E. C.; Jongeward, G. A.; Wolynes, P. G. *J. Chem. Phys.* **1983**, *79*, 6277−6281.
(53) Cline, R. E.; Wolynes, P. G. *J. Chem. Phys.* **1987**, *86*, 3836.
(54) Jarrell, M.; Gubernatis, J. E. *Phys. Rep.* **1996**, *269*, 133.
(55) Galliccio, E.; Berne, B. J. *J. Chem. Phys.* **1996**, *105*, 7064−7078.
(56) Gillan, M. J. *J. Phys. C* **1987**, *20*, 3621−3641.
(57) Voth, G. A.; Chandler, D.; Miller, W. H. *J. Chem. Phys.* **1989**, *91*, 7749−7760.
(58) Sun, Y.-C.; Voth, G. A. *J. Chem. Phys.* **1993**, *98*, 7451−7458.

(59) Cao, J.; Voth, G. A. *J. Chem. Phys.* **1994**, *100*, 5106.
(60) Cao, J.; Voth, G. A. *J. Chem. Phys.* **1994**, *101*, 6157.
(61) Voth, G. A. *Adv. Chem. Phys.* **1996**, *XCIII*, 135.
(62) Gerber, R. B. *Chem. Rev.* **1999**, *99*, 1583−1606.
(63) Makri, N. *Adv. Chem. Phys.* **1999**.
(64) Makri, N. *Comput. Phys. Commun.* **1991**, *63*, 389−414.
(65) Mukamel, S. *Principles of nonlinear optical spectroscopy*; Oxford University Press: New York, 1995.
(66) Feynman, R. P.; Hibbs, A. R. *Quantum Mechanics and Path Integrals*; McGraw-Hill: New York, 1965.
(67) Schulman, L. S. *Techniques and applications of path integration*; John Wiley and Sons: New York, 1981.
(68) Batista, V. S.; Miller, W. H. *J. Chem. Phys.* **1998**, *108*, 498−510.
(69) Sun, X.; Miller, W. H. *J. Chem. Phys.* **1997**, *106*, 916−927.
(70) Ovchinnikov, M.; Apkarian, V. A. *J. Chem. Phys.* **1997**, *105*, 10312.
(71) Ovchinnikov, M.; Apkarian, V. A. *J. Chem. Phys.* **1998**, *108*, 2277−2284.
(72) Sepulveda, M. A.; Mukamel, S. *J. Chem. Phys.* **1995**, *102*, 9327−9344.
(73) Sepulveda, M. A.; Grossmann, F. *Adv. Chem. Phys.* **1996**, *XCVI*, 191.
(74) Spencer, C. F.; Loring, R. F. *J. Chem. Phys.* **1996**, *105*, 6596.
(75) Pentidis, S. A.; Loring, R. F. *Chem. Phys. Lett.* **1998**, *287*, 217.
(76) Jungwirth, P.; Fredj, E.; Gerber, R. B. *J. Chem. Phys.* **1996**, *104*, 9332−9339.
(77) Jungwirth, P.; Fredj, E.; Gerber, R. B. *J. Chem. Phys.* **1997**, *107*, 8963.
(78) Ovchinnikov, M.; Apkarian, V. A. *J. Chem. Phys.* **1997**, *106*, 5775−5778.
(79) Potter, E. D.; Liu, Q.; Zewail, A. H. *Chem. Phys. Lett.* **1992**, *200*, 605.
(80) Wan, C.; Gupta, M.; Baskin, J. S.; Kim, Z. H.; Zewail, A. H. *J. Chem. Phys.* **1997**, *106*, 4353−4356.
(81) Whitnell, R. M.; Wilson, K. R.; Yan, Y.; Zewail, A. H. *J. Mol. Liq.* **1994**, *61*, 153−165.
(82) Liu, L.; Guo, H. *J. Chem. Phys.* **1995**, *103*, 7851.
(83) Ka, J.; Shin, S. *Chem. Phys. Lett.* **1997**, *269*, 227.
(84) Yan, Y.; Whitnell, R. M.; Wilson, K. R. *Chem. Phys. Lett.* **1992**, *193*, 402−412.
(85) Swope, W. C.; Andersen, H. C.; Berens, P. H.; Wilson, K. R. *J. Chem. Phys.* **1982**, *76*, 637.
(86) Feit, M. D.; Fleck, J. A.; Steiger, A. *J. Comput. Phys.* **1982**, *47*, 412.